Contribution from the Dipartimento di Chimica, University of Florence, 50144 Firenze, Italy, and Centre d'Etudes Nucleaires, Grenoble, France

Moderate Ferromagnetic Exchange between Copper(II) and a Nitronyl Nitroxide in a Square-Pyramidal Adduct. MO Interpretation of the Mechanism of Exchange in Copper(II)–Nitroxide Complexes

A. Caneschi,[1a] D. Gatteschi,*[1a] A. Grand,[1b] J. Laugier,[1b] L. Pardi,[1a] and P. Rey*[1b]

Received May 7, 1987

Bis(trifluoroacetylacetonato)copper(II), $Cu(tfac)_2$, reacts with the nitronyl nitroxide radical 2,4,4,5,5-pentamethyl-4,5-dihydro-1*H*-imidazolyl-1-oxy 3-oxide, NITMe, to yield a square-pyramidal adduct of formula $Cu(tfac)_2$·NITMe. The X-ray crystal structure shows that it crystallizes in the space group $P\bar{1}$, with a = 10.119 (5) Å, b = 12.159 (6) Å, c = 11.814 (5) Å, α = 115.13 (1)°, β = 85.30 (1)°, γ = 68.42 (1)°, and Z = 2. The distance of the copper ion from the oxygen of the axial NITMe is 2.303 Å. The magnetic data shows that the coupling is ferromagnetic, with a singlet–triplet splitting of 65 ± 5 cm^{-1}. Structural–magnetic correlations for copper(II)–nitroxide complexes have been established through extended Hückel calculations.

Introduction

We have recently started a thorough program of characterization of the structure and of the magnetic properties of compounds containing coupled paramagnetic metal ions and stable organic radicals, such as the nitroxides.[2-5] We have shown that many different coupling mechanisms can be observed, ranging from strong antiferromagnetic[6,7] to ferromagnetic.[3,7] It is especially compounds of the latter type that are of interest, because they might be used to design molecular ferromagnets.

Ferromagnetic coupling up to now has been observed in adducts of copper(II) hexafluoroacetylacetonate with various nitroxides in the axial position, the maximum reported coupling being −26 cm^{-1}. Although this can be considered to be encouraging in order to synthesize bulk ferromagnets, the value is still too low. In order to proceed further it would be useful to find a relation between the observed coupling and the electronic structure of the complexes, but this has not yet emerged because up to now J has been found not to vary significantly for the reported complexes.

We have now synthesized a new adduct of copper trifluoroacetylacetonate ($Cu(tfac)_2$) with the nitronyl nitroxide 2,4,4,5,5-pentamethyl-4,5-dihydro-1*H*-imidazolyl-1-oxy 3-oxide (NITMe) of formula $Cu(tfac)_2$·NITMe, which shows a substantially larger ferromagnetic coupling than all the previous ones, J being close to 65 cm^{-1}. Here we report the crystal structure of this compound and use extended Hückel calculations to discuss the mechanism of exchange in copper–nitroxide complexes.

Experimental Section

Synthesis of the Complex. $Cu(tfac)_2$ was prepared by mixing a water solution of $Cu(CH_3COO)_2·H_2O$ with the stoichiometric amount of trifluoroacetylacetone. A violet precipitate appeared immediately, which was filtered, washed with cold water, and dried in vacuum over silica gel. The NITMe radical was prepared as previously described.[8] One millimole of the copper(II) salt was dissolved in 100 mL of dry *n*-heptane; the solution was boiled for 10 min and then cooled down to 60 °C and mixed under stirring at 60° C for 10 min with 1 mmol of NITMe. The solution was stored at room temperature for 18 h and filtered to separate violet crystals of unreacted $Cu(tfac)_2$; then it was stored at −2 °C for 24 h, and nice wine red crystals suitable for an X-ray diffraction study were collected. The compound analyzed satisfactorily for $Cu(tfac)_2$·NITMe. Anal. Calcd for $CuC_{18}F_6H_{23}N_2O_6$: Cu, 11.75; C, 39.36; H, 4.26; N, 5.18. Found: Cu, 11.7; C, 39.83; H, 4.47; N, 5.14.

Table I. Crystal Data and Experimental Parameters

A. Crystal Data			
formula	$C_{18}H_{23}F_6O_6N_2Cu$	V, Å^3	1173.7
fw	540.9	Z	2
a, Å	10.119 (5)	d(calcd), g/cm^3	1.53
b, Å	12.159 (6)	cryst syst	triclinic
c, Å	11.814 (5)	space group	$P\bar{1}$
α, deg	115.13 (1)	cryst size, mm	0.20 × 0.25 × 0.30
β, deg	85.30 (1)	linear abs (μ), mm^{-1}	0.5
γ, deg	68.42 (1)		

B. Experimental Data	
temp	20 °C
radiation	takeoff angle: 6°
	wavelength: 0.7107 Å (Mo Kα)
	monochromator: graphite
Bragg angle	$2 < \theta < 30°$
scan	mode: ω
	range: $(0.8 + 0.35 \tan \theta)°$
	speed: from 0.6 to 4 deg/min
detector window	height: 4 mm
	width: $2.4 + 3.0 \tan \theta$ mm
test reflcns	(044), (30$\bar{3}$), (65$\bar{2}$)
measd reflcns	$-15 < h < 15$, $-17 < k < 17$, $0 < l < 17$
	tot. no.: 7124
	no. with $F > 4\sigma(F)$: 3495
refinement	R: 0.053
	R_w: 0.058

Magnetic Susceptibility Measurements. Magnetic susceptibility measurements were performed between 6 and 300 K by using an SHE superconducting SQUID susceptometer at a field strength of 0.5 T. Data were corrected for the magnetization of the sample holder. Diamagnetic contributions were estimated from Pascal constants.

X-ray Structure Determination. Preliminary Weissenberg photographs taken for a small crystal (0.22 × 0.19 × 0.26 mm) exhibited a spot pattern only compatible with a triclinic space group. The same crystal was mounted on an Enraf-Nonius CAD-4 diffractometer. The orientation matrix for data collection and the unit cell parameters were obtained by using the automated routines incorporated in the Enraf-Nonius package. Intensities of 3 standard reflections were measured after every 100 reflections. The data were corrected for standard decay and Lorentz and polarization effects but not for absorption. Crystal data and experimental parameters are tabulated in Table I.

The structure was solved by conventional Patterson and Fourier methods using the SHELX-76 package.[9,10] The final refinement model included anisotropic thermal parameters for all non-hydrogen atoms. Hydrogen atoms were included at fixed, idealized positions but not refined. There was evidence of a degree of disorder and/or high thermal

(1) (a) University of Florence. (b) Centre d'Etudes Nucleaires.
(2) Benelli, C.; Gatteschi, D.; Zanchini, C. *Inorg. Chem.* **1984**, *23*, 798.
(3) Bencini, A.; Benelli, C.; Gatteschi, D.; Zanchini, C. *J. Am. Chem. Soc.* **1984**, *106*, 5813.
(4) Grand, A.; Rey, P.; Subra, R. *Inorg. Chem.* **1983**, *22*, 391.
(5) Benelli, C.; Gatteschi, D.; Latour, J. M.; Rey, P. *Inorg. Chem.* **1986**, *25*, 4242.
(6) Laugier, J.; Rey, P.; Benelli, C.; Gatteschi, D.; Zanchini, C. *J. Am. Chem. Soc.* **1986**, *108*, 6931.
(7) Caneschi, A.; Gatteschi, D.; Rey, P. *J. Chem. Soc. Faraday Trans. 1*, in press.
(8) Ullman, E. F.; Osiecki, J. H.; Boocock, D. G. B.; Darcy, R. *J. Am. Chem. Soc.* **1972**, *94*, 7049.
(9) Stewart, J. M.; Kundall, F. A.; Baldwin, J. C. "X-ray 72 System of Programs"; Technical Report TR 192; University of Maryland: College Park, MD, 1972. Sheldrick, G. "SHELX 76 System of Computing Programs"; University of Cambridge: Cambridge, England, 1976. Johnson, C. K. "ORTEP"; Report ORNL 3794; Oak Ridge National Laboratory: Oak Ridge, TN, 1965.
(10) *International Tables of X-ray Crystallography*; Kynoch: Birmingham, England, 1974; Vol. IV, p 71.

0020-1669/88/1327-1031$01.50/0

Table II. Positional Parameters ($\times 10^4$)[a]

	x	y	z	B_{eq}, Å^2
Cu	3745 (1)	5366 (1)	2102 (1)	4.71
O1	5833 (3)	4339 (3)	1298 (3)	5.30
O2	3683 (3)	6922 (3)	1991 (3)	5.13
O3	1626 (3)	6328 (3)	2762 (3)	5.96
O4	3731 (3)	3684 (3)	1846 (3)	5.61
O5	4195 (3)	6092 (3)	4109 (3)	5.40
O6	612 (4)	7599 (4)	7776 (4)	9.87
N1	3212 (4)	6888 (3)	5223 (4)	4.53
N2	1627 (4)	7612 (4)	6987 (4)	6.42
F1	3532 (4)	8703 (3)	1075 (4)	8.92
F2	5628 (4)	8502 (3)	1297 (4)	10.70
F3	3865 (5)	9341 (3)	2938 (4)	8.93
F4	−1175 (4)	7492 (4)	2637 (5)	21.77
F5	−1770 (3)	6260 (3)	3132 (4)	10.98
F6	−1138 (4)	7681 (4)	4453 (5)	10.58
C1	6689 (5)	4716 (5)	901 (4)	3.83
C2	8293 (5)	3674 (5)	232 (5)	7.33
C3	6263 (5)	6001 (5)	1014 (5)	4.80
C4	4817 (5)	6988 (4)	1568 (4)	3.44
C5	4454 (7)	8393 (5)	1712 (6)	5.29
C6	785 (5)	5775 (4)	2734 (5)	5.15
C7	−552 (6)	6788 (6)	3256 (7)	8.03
C8	1148 (5)	4433 (4)	2345 (5)	5.41
C9	2626 (6)	3456 (5)	1938 (5)	4.47
C10	2921 (6)	2027 (5)	1619 (6)	7.84
C11	2767 (6)	8380 (4)	5977 (5)	5.07
C12	1668 (8)	8990 (6)	5252 (7)	7.89
C13	3989 (8)	8681 (6)	5851 (7)	9.52
C14	1828 (6)	8790 (5)	7286 (5)	6.75
C15	2921 (9)	8684 (8)	8193 (7)	5.02
C16	558 (9)	10053 (6)	8019 (8)	27.44
C17	2431 (5)	6531 (5)	5829 (5)	5.19
C18	2559 (6)	5135 (5)	5324 (6)	5.91

[a] Standard deviations in the last significant digits are in parentheses.

Table III. Bond Lengths (Å)[a]

Cu–O1	1.910 (2)	C4–C5	1.537 (8)
Cu–O2	1.930 (4)	C6–C7	1.526 (6)
Cu–O3	1.918 (2)	C6–C8	1.380 (6)
Cu–O4	1.942 (4)	C8–C9	1.403 (6)
Cu–O5	2.303 (3)	C9–C10	1.515 (8)
O5–N1	1.286 (4)	C11–C12	1.615 (10)
O6–N2	1.268 (7)	C11–C13	1.426 (11)
O1–C1	1.260 (7)	C11–C14	1.516 (8)
O2–C4	1.257 (6)	C14–C15	1.611 (10)
O3–C6	1.259 (7)	C14–C16	1.413 (6)
O4–C9	1.254 (7)	C17–C18	1.490 (8)
N1–C11	1.499 (5)	F1–C5	1.295 (8)
N1–C17	1.322 (8)	F2–C5	1.321 (8)
N2–C14	1.476 (8)	F3–C5	1.310 (6)
N2–C17	1.349 (4)	F4–C7	1.319 (11)
C1–C2	1.514 (5)	F5–C7	1.295 (8)
C1–C3	1.401 (8)	F6–C7	1.281 (7)
C3–C4	1.376 (5)		

[a] Standard deviations in the last significant digits are in parentheses.

motion of the methyl groups of the nitroxyl fragment. Difference Fourier maps did not yield a second well-resolved and internally consistent set of methyl carbon atoms. These maps clearly indicated that the refined positions accounted for the majority (>70%) of the electron density expected. Therefore no provision for disorder was introduced in the refinement. This does not seriously affect the chemically significant features of the structure.

The positional coordinates of the non-hydrogen atoms are given in Table II; anisotropic thermal parameters (Table SI) and a listing of the F_o and F_c values (Table SII) are deposited as supplementary material.

Calculations. The extended Hückel calculations were performed on an IBM 4361/3 computer. The parameters used in the calculations are reported in Table SIII. In the axial case the CuF_4^{2-} moiety has tetragonal symmetry, with a Cu–F bond of 2 Å; the H_2NO moiety has C_{2v} symmetry and the following structural parameters: N–O = 1.276 Å; N–H = 1 Å. The angular parameters are the three Euler angles ψ, θ and ϕ, defined by starting with the H_2NO moiety lying on the XZ plane and then rotating the nitroxide by an angle ψ around Z, by θ around Y, and finally by ϕ around Z. In the equatorial case the nitroxide model is still

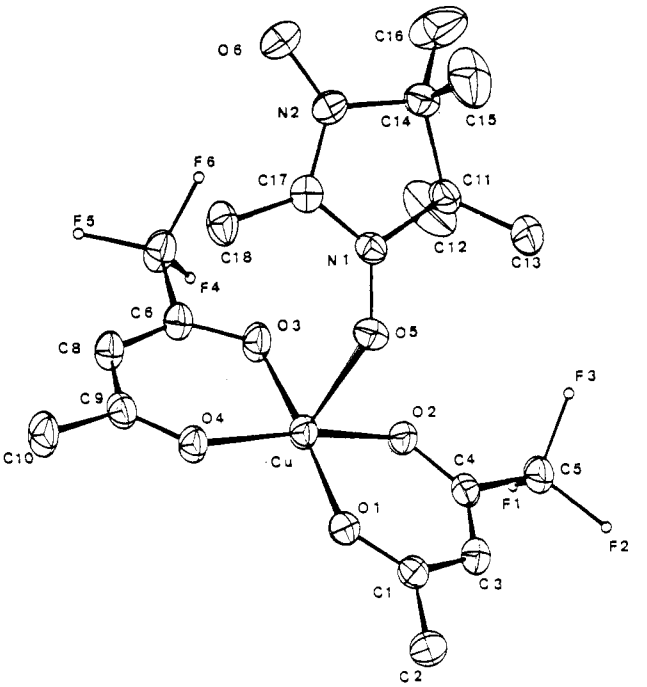

Figure 1. ORTEP view of the molecular structure of $Cu(tfac)_2 \cdot NITMe$.

Table IV. Bond Angles (deg)[a]

O1–Cu–O2	93.0 (1)	O3–C6–C8	129.2 (4)
O1–Cu–O3	175.0 (1)	C7–C6–C8	118.1 (5)
O1–Cu–O4	87.0 (1)	F4–C7–F5	104.9 (5)
O1–Cu–O5	89.0 (1)	F4–C7–F6	104.6 (5)
O2–Cu–O3	87.2 (1)	F4–C7–C6	110.8 (5)
O2–Cu–O4	167.6 (1)	F5–C7–F6	108.6 (5)
O2–Cu–O5	93.2 (1)	F5–C7–C6	115.4 (5)
O3–Cu–O4	91.7 (1)	F6–C7–C6	111.7 (5)
O3–Cu–O5	95.9 (1)	C6–C8–C9	121.6 (5)
O4–Cu–O5	99.2 (1)	O4–C9–C8	124.8 (5)
O5–N1–C11	123.0 (4)	O4–C9–C10	117.1 (4)
O5–N1–C17	125.6 (3)	C8–C9–C10	118.1 (5)
C11–N1–C17	111.3 (3)	N1–C11–C12	103.1 (4)
O6–N2–C14	123.5 (3)	N1–C11–C13	112.3 (3)
O6–N2–C17	124.7 (5)	N1–C11–C14	102.4 (4)
C14–N2–C17	111.5 (4)	C12–C11–C13	107.2 (6)
C2–C1–C3	118.4 (5)	C12–C11–C14	107.6 (4)
C1–C3–C4	122.0 (5)	C13–C11–C14	122.6 (5)
O2–C4–C3	129.2 (5)	N2–C14–C11	102.3 (3)
O2–C4–C5	112.1 (3)	N2–C14–C15	102.8 (5)
C3–C4–C5	118.7 (5)	N2–C14–C16	113.6 (6)
F1–C5–F2	106.5 (6)	C11–C14–C15	106.8 (5)
F1–C5–F3	107.7 (4)	C11–C14–C16	121.9 (6)
F1–C5–C4	112.1 (5)	C15–C14–C16	107.7 (5)
F2–C5–F3	105.7 (5)	N1–C17–N2	109.9 (4)
F2–C5–C4	113.6 (4)	N1–C17–C18	125.1 (3)
F3–C5–C4	110.9 (5)	N2–C17–C18	125.0 (5)
O3–C6–C7	112.7 (4)		

[a] Standard deviations in the last significant digits are in parentheses.

H_2NO; for the square-planar complex the metal fragment is taken simply as CuF_3^-, with the three fluoride ligands on three vertices of a square in order to have as high a symmetry as possible. The angular parameters are defined analogously to the axial case, the only difference being that the ψ and ϕ rotations are performed around the X axes instead of Z. For the trigonal-bipyramidal case the geometric parameters are defined in the same way by substituting the CuF_3^- moiety of the square planar complex, with the CuF_4^{2-} one, in which two fluoride ions lie along the Z axes and two other occupy two of the equatorial positions of a trigonal bipyramid, and third being occupied by the oxygen of the nitroxide placed along the X axes.

Description of the Structure

Figure 1 shows all the bonding interactions important for the metal ion in this compound. The relevant bond distances and angles are given in Tables III and IV. The bonding pattern of the copper(II) ion closely approximates a square pyramid, with

Table V. Structural and Magnetic Parameters for Axially Coordinated Copper(II)–Nitroxide Complexes

compd[b]	R, Å	ψ, deg	θ, deg	ϕ, deg	J, cm^{-1}	ref
Cu(hfac)$_2$TEMPOL	2.439	72.3	9.9	85.4	13	11
Cu(pacTEMPOL)$_2$[a]	2.583	30.2	21.5	87.6	19	4
Cu(pacTEMPOL)$_2$[a]	3.157	55.3	40.5	50.1	19	4
Cu(proxFORMIL)$_2$	2.606	84.3	46.4	71.8	21	12
Cu(hfac)$_2$·NITMe[a]	2.341	70.8	47.7	73.8	26	13
Cu(hfac)$_2$·NITMe[a]	2.431	76.4	58.4	65.6	26	13
Cu(hfac)$_2$(NITPh)$_2$	2.393	72.0	42.3	70.8	9.8	14
Cu(tfac)$_2$·NITMe	2.303	80.5	54.2	90.0	65	*c*

[a] Two different copper–nitroxide distances are observed in the cell. [b] hfac = hexafluoroacetylacetonato, tfac = trifluoroacetylacetonato, tcact = trichloroacetato, TEMPOL = 4-hydroxy-2,2,6,6-tetramethylpiperidinyl-1-oxy, TEMPO = 2,2,6,6-tetramethylpiperidinyl-1-oxy, pacTEMPOL = (1-oxy-2,2,6,6-tetramethylpiperidin-4-yl)pivaloylacetato, proxFORMIL = 1-oxy-3-formyl-4-oxo-2,2,5,5-tetramethylpyrrolidine, NITMe = 2,4,4,5,5-pentamethyl-4,5-dihydro-1*H*-imidazolyl-1-oxy 3-oxide, NITPh = 2-phenyl-4,4,5,5-tetramethyl-4,5-dihydro-1*H*-imidazolyl-1-oxy 3-oxide, and PROXYL = 2,2,5,5-tetramethylpiperidinyl-1-oxy. [c] This work.

the four oxygen atoms of the tfac ligands in the basal plane and the nitroxyl oxygen atom axially coordinated. In the basal plane, the two oxygen atoms vicinal to the trifluoro methyl groups have metal-bonding distances shorter than the two others by ca. 0.02 Å. The Cu(II)–O(nitroxyl) bond length is 2.303 Å; thus, the compound is, among all the structurally characterized axially coordinated copper–nitroxyl complexes,[4,11-14] the more tightly bound. The copper ion is displaced from the basal plane of the square pyramid toward the O(nitroxyl) atom (0.14 Å).

In the Cu(tfac)$_2$ fragment, the trifluoromethyl groups show the usual preferred orientation in which one fluorine atom lies in the plane of the chelate ring at a maximum distance from the nearest coordinating oxygen atom.[15]

The nitronyl nitroxide moiety exhibits the expected planar O5–N1–C17–N2–O6 fragment from which the tetramethylethylene fragment is slightly twisted out.[16]

The shortest intermolecular contact involving the paramagnetic centers is found between the two oxygen atoms of the nitroxides which are not bound to the metal ion (O6–O'6 = 5.549(7) Å). This large separation allows us to consider this complex in the solid state as a discrete mononuclear copper complex, although it does not rule out a possible weak intermolecular interaction (see below).

Magnetic Data

The temperature dependence of the magnetic susceptibility in the form χT vs T is shown in Figure 2. The room-temperature value, 0.877 emu mol^{-1} K, is only slightly higher than that expected for two noncoupled $S = {}^1/_2$ free spins. When the temperature is lowered, χT increases and reaches a maximum of 1.017 emu mol^{-1} K at ca. 30 K. This value agrees well with a ground S = 1 spin state. At lower temperatures χT decreases, presumably due to antiferromagnetic intermolecular interactions.

The experimental χT values were first fit with a Bleaney–Bowers equation,[17] not including temperature-independent paramagnetism (TIP), and the results were only moderately satisfactory.

A second fit including TIP was attempted, and in this case the agreement was satisfactory. The values of the parameters are the following: g = 2.0119 (1) and J = −71.51 (1) cm^{-1}, for TIP = 2.27 × 10^{-4} emu mol^{-1}. In this minimization we did not include the points below 13 K, because they are clearly affected by intermolecular interactions. The agreement factor, defined as $\sum_i \Delta(\chi T)_i^2 / \sum_i (\chi_{oss} T)_i^2$, is 3.56 × 10^{-3}.

Attempts were made also to take into account the decrease in the χT values at lower temperatures, by including a J' coupling constant between two Cu(tfac)$_2$·NITMe moieties. The rationale for this would be the relatively short contact between the oxygen atoms of two N–O groups of two NITMe moieties seen in the crystal structure. In this case all the points were introduced in the fitting procedure. The best-fit parameters are g = 2.0351 (3), J = −60.4 (2) cm^{-1}, and J' = 0.38 (3) cm^{-1}, for a TIP = 2.27 × 10^{-4} emu mol^{-1}. The agreement factor is 3.72 × 10^{-3}. It must be noted that the addition of a second exchange parameter increases the agreement factor slightly, but the number of experimental points is higher than in the two-parameter fit. The value of J' = 0.38 cm^{-1}, attributed to the interaction of two oxygen atoms at 5.549 (7) Å, should be compared to J' = 15.05 (1) cm^{-1} observed[6] in CuCl$_2$(NITPh)$_2$, where the shortest distance between the two interacting NITPh moieties is 3.56 Å.

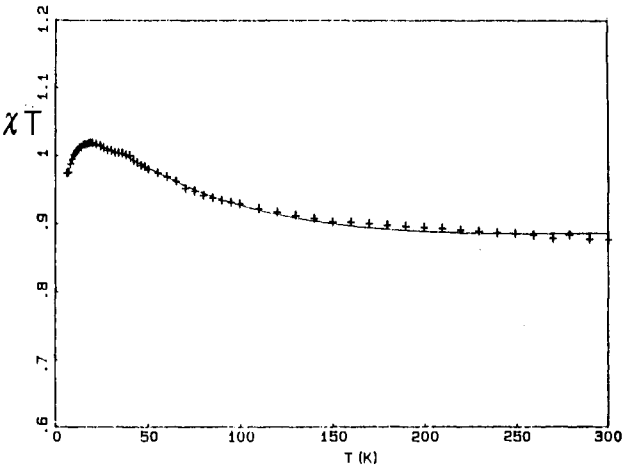

Figure 2. Variation of the χT product with temperature for Cu(tfac)$_2$·NITMe in the range 6–300 K. The curve represents the best fit of the experimental data obtained with J = −71.51 (1) cm^{-1} and g = 2.0119.

The presence of intermolecular interactions can be confirmed by the EPR spectra, which do not show the expected triplet structure, but only one broad band is observed, centered at g = 2.15, with peak to peak width of 480 G, which may be explained by the overlap of different transitions including the total spin states S = 1, 2 formed by triplet–triplet interactions. The magnetic data therefore show that a moderate ferromagnetic coupling is operative between copper and NITMe. The exact value of J cannot be determined, because of the intrinsic lack of precision associated with the fit of two $S = {}^1/_2$ spin coupled ferromagnetically.[18,19] However 65 ± 5 cm^{-1} seems to be a reasonable range from the above analysis. In Table V we collect the available data of similar complexes, which will be discussed in the next section.

Extended Hückel Calculations

In order to understand which are the factors responsible for the coupling in copper(II)–nitroxide complexes, we have performed extended Hückel calculations. Hay et al.[20] decomposed the iso-

(11) Anderson, O. P.; Kuechler, T. C. *Inorg. Chem.* **1980**, *19*, 1417.
(12) Laugier, J.; Ramasseul, R.; Rey, P.; Espie, J. C.; Rassat, A. *Nouv. J. Chim.* **1983**, *7*, 11.
(13) Caneschi, A.; Gatteschi, D.; Laugier, J.; Rey, P. *J. Am. Chem. Soc.* **1987**, *109*, 2191.
(14) Gatteschi, D.; Laugier, J.; Rey, P.; Zanchini, C. *Inorg. Chem.* **1987**, *26*, 938.
(15) Belford, R. C. E.; Fenton, D. E.; Truter, M. R. *J. Chem. Soc., Dalton Trans.* **1974**, *1*, 17.
(16) Wong, W. K. W. Thesis, Louisiana State University, 1974.
(17) Bleaney, B.; Bowers, K. D. *Proc. R. Soc. London* **1952**, *451*, A214.
(18) Hatfield, W. E. *Inorg. Chem.* **1983**, *22*, 833.
(19) Carlin, R. L.; Burriel, R.; Corneliesse, R. M.; van Duyneveldt, A. J. *Inorg. Chem.* **1983**, *22*, 891.

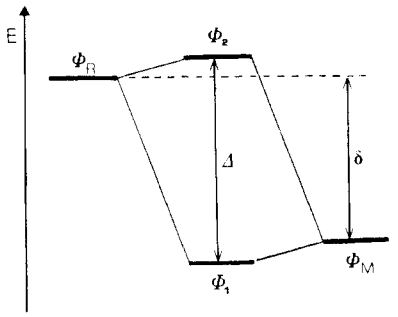

Figure 3. Qualitative molecular orbital diagram for the interaction between the metal and the nitroxide magnetic orbitals.

tropic exchange into ferromagnetic, J_F, and antiferromagnetic, J_{AF}, components and used the extended Hückel formalism to evaluate the antiferromagnetic component of the isotropic exchange in a series of symmetric dinuclear metal complexes. In order to use the same model for copper(II)–nitroxide complexes, some modifications must be introduced.

First of all, since the exchange is presumably of the direct type, it is very useful to employ the method of fragments, including in one fragment the nitroxide and in the other the metal complex. J_{AF} may then be estimated by the interaction of the magnetic orbitals of the two fragments. In Figure 3 is plotted a qualitative scheme of a possible interaction between the metal and the nitroxide magnetic orbitals. Φ_M is the "metal" orbital, actually a molecular orbital delocalized on the metal fragment, and analogously Φ_R is the radical orbital. For the compounds in which the interaction between the magnetic orbitals is relatively weak (the metal–radical overlap is small, and the energy separation between the two orbitals is large), the molecular orbitals Φ_1 and Φ_2 will be mainly localized on the metal and on the radical fragment respectively. Under these conditions J_{AF} must be proportional[21] to $(\Delta^2 - \delta^2)^{1/2}S$, where S is the overlap integral between the magnetic orbitals, as defined in Figure 3. Since $(\Delta^2 - \delta^2)^{1/2}$ on its turn is expected to be proportional to the overlap of the two magnetic orbitals, in a series of analogous compounds, J_{AF} is determined by the variation of the squared overlap[22] between the magnetic orbitals. Therefore we use this criterion as a guidance in the rationalization of the magnetic coupling in copper(II)–radical complexes. We neglect completely the ferromagnetic component, which cannot be calculated within the extended Hückel model, and try to verify if the assumption that J_F is a slowly varying function in a series of complexes, established for coupled copper(II) dimers, holds also for the copper–radical species.

We performed sample calculations on two different series, one in which the nitroxide occupies an axial site of a square pyramid, and the other in which the nitroxide is in an equatorial site of either a square-planar, a square-pyramidal, or a trigonal-bipyramidal complex.

Axial Complexes. In the axial case we have taken into consideration as geometric parameters, the copper–oxygen distance R and the Euler angles ψ, θ, and ϕ defined in the Experimental Section. When the Cu–O bond is orthogonal to the equatorial plane, the angle ϕ is determined by the angle of the projection of the O–N bond in the XY plane with the X axis; θ is the angle of the O–N bond with the perpendicular to the plane, and ψ is the dihedral angle between the Cu–O–N and the nitroxide planes.

For the sake of simplicity we used CuF_4^{2-} and H_2NO as representative fragments. These fragments are only poor approximations to the true molecules, but since we are interested only in relative variations of the overlap, what is really important is to have simple molecular fragments that can give an idea of how the geometrical parameters can affect the overlap. When the two

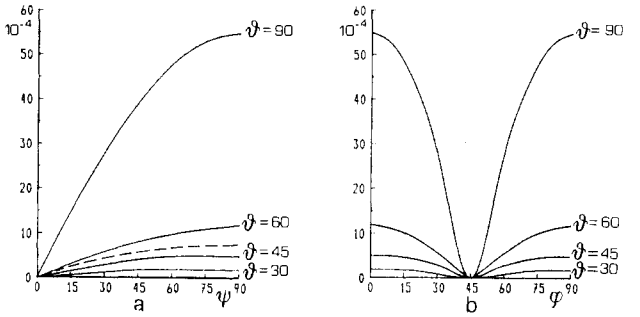

Figure 4. Variation of the absolute value of the overlap, between magnetic orbitals, in axially coordinated copper–nitroxide complexes: (a) variation of S with ψ and θ for $\phi = 0°$; (b) variation of S with ϕ and θ for $\psi = 90°$.

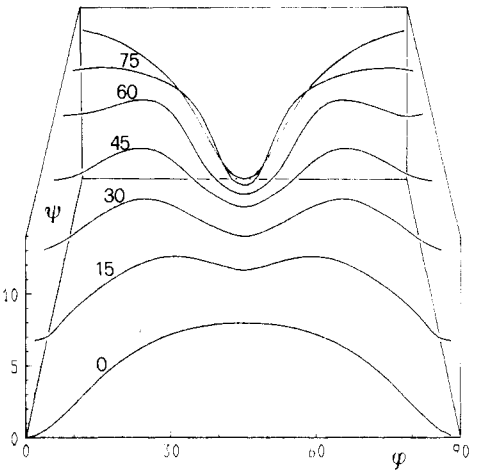

Figure 5. Variation of the absolute value of the overlap, between magnetic orbitals, in axially coordinated copper–nitroxide complexes, with ψ and ϕ for $\theta' = 60°$.

moieties are allowed to interact, at a copper–oxygen distance of 2 Å, the two orbitals show only a very small overlap. In Figure 4 we show the variation of the absolute value of the overlap S, with the angular parameters.

For $\theta = 0°$, the Cu–O–N angle is 180°, therefore the π^* and $d_{x^2-y^2}$ orbitals are orthogonal to each other irrespective of the ψ and ϕ angles. In this case the antiferromagnetic contribution is zero, and a moderate ferromagnetic coupling can be developed. It can be expected that the shorter the copper–oxygen distance, the larger the coupling.

When θ is different from zero, the ψ and ϕ angles become important. When $\phi = 0°$, an increase in ψ, from 0 to 90°, causes an increase of the overlap (Figure 4a). The effect is much more pronounced at $\theta = 90°$ than at smaller angles. In practice S does not become important until θ is fairly close to 90°, a value that does not seem to be very reasonable on steric grounds and indeed has never been observed experimentally. The reported values of θ seem to cluster around 50°, with one value as low as 9.9° and the largest so far reported at 58.4° (Table V).

The effect of varying ϕ, for $\psi = 90°$, shows a deep minimum for $\phi = 45°$ (Figure 4b), because in this case the lobe of π is pointing between the lobes of $d_{x^2-y^2}$, thus making the two orbitals orthogonal. In Figure 5 we show the dependence of the overlap on the ψ and ϕ angles for a constant value of θ.

In order to check the influence of the nature of the nitroxides on the magnetic coupling, the same calculations were performed also by using the following model of the nitroxide:

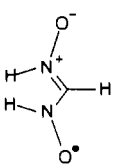

(20) Hay, P. J.; Thibeault, J. C.; Hoffman, R. *J. Am. Chem. Soc.* **1975**, *97*, 4884.
(21) Kahn, O. *Inorg. Chim. Acta* **1982**, *62*, 3.
(22) Kahn, O. *Magneto-Structural Correlations in Exchange Coupled Systems*; Willet, R. D.; Gatteschi, D.; Kahn, O., Eds.; D. Reidel: Dordrecht, Holland, 1985.

Table VI. Structural and Magnetic Parameters for Diamagnetic Equatorially Coordinated Copper(II)–Nitroxide Complexes

compd	R, Å	ψ, deg	θ, deg	ϕ, deg	ref
(a) Square-Planar or Square-Pyramidal Complexes					
$Cu(hfac)_2NITPh$[a]	1.955	88.4	59.0	56.5	14
$Cu(hfac)_2TEMPO$	1.920	84.7	56.2	63.7	23
$CuCl_2(NITPh)_2$	1.980	64.1	56.3	67.5	6
(b) Trigonal-Pyramidal Complexes					
$Cu(hfac)_2NITPh$[a]	1.948	80.2	59.8	41.9	14
$Cu(tcact)_2TEMPO$[b]	1.942	81.5	56.5	7.0	24
$Cu(tcact)_2TEMPO$[b]	1.950	85.8	56.2	1.9	24
$Cu(tcact)_2PROXYL$[b]	1.970	79.4	47.4	75.8	25
$Cu(tcact)_2PROXYL$[b]	1.961	85.2	54.0	11.7	25

[a] Two different coordination geometries are observed in the cell. [b] Two copper–Nitroxide moieties in the cell.

This model is a closer approximation to the nitronyl nitroxide. These calculations revealed that the main effect of changing the nitroxide is a lowering of the overlap. This is illustrated by the dotted line in Figure 4a, representing the variation of the overlap in the nitronyl nitroxide complex, for $\theta = 60°$ and $\phi = 0°$. As far as the overlap is concerned, in nitronyl nitroxides the antiferromagnetic component of J must be smaller than in the corresponding nitroxides.

In conclusion, for a given θ, the largest values of J_{AF} must be expected (i) for ψ close to 90° and ϕ close to 0 or 90° or (ii) for ψ close to 0° and ϕ close to 45°. An increase in θ tends to give larger overlap.

The comparison with experimental data can be done by using Table V, where we collected the available structures and magnetic data for axial copper–nitroxide complexes. In order to discuss these data it must be considered that all the complexes show a ferromagnetic coupling and that accurate values of the exchange constants are difficult to obtain in these cases. Further in several complexes two different species are present, making any structural–magnetic correlation difficult, because at best the "average" coupling constant can be obtained from one experiment. Finally different nitroxides have been used, which can affect to a large extent the coupling, according to their relative delocalization.

A meaningful comparison may start from $Cu(tfac)_2$·NITMe and $Cu(hfac)_2(NITPh)_2$,[14] which have rather similar ligands, and largely different coupling constants. The shorter distance observed in $Cu(tfac)_2$·NITMe is expected to make any interaction, either ferro- or antiferromagnetic, more intense than in $Cu(hfac)_2(NITPh)_2$. As regards the overlap, all the angles concur in suggesting a higher value for $Cu(tfac)_2$·NITMe than for $Cu(hfac)_2(NITPh)_2$. In fact, θ and ψ are all larger for the former, with ψ and ϕ close to 90°. From Figures 4 and 5 we learn that, in this range of values, larger angles mean larger overlap. Therefore the conclusion must be that the antiferromagnetic component of the coupling constant, J_{AF}, must be larger for $Cu(tfac)_2$·NITMe than for $Cu(hfac)_2(NITPh)_2$. Since the experimental data show that the coupling constant is more ferromagnetic for $Cu(tfac)_2$·NITMe than for $Cu(hfac)_2(NITPh)_2$, we must conclude that for this series of complexes the variations of J are not determined by variations in J_{AF}, but rather by J_F. Indeed the calculated overlaps are always very small, thus making J_{AF} very small in any case. Therefore we conclude that the short Cu–O distance in $Cu(tfac)_2$·NITMe is actually responsible for a larger J_F than in the other members of the series and consequently for a more intensive ferromagnetic interaction.

The same conclusions are reached by also performing some calculations on more accurate models of the above molecules.

Equatorial Complexes. In the complexes in which the nitroxide occupies an equatorial position, a notable reduction in the distance between the metal and the oxygen of the nitroxide, in comparison with the axial case, is observed, as shown in Table VI. Representative of this structural type is the complex $Cu(hfac)_2NITPh$, whose structure has two different molecules in the asymmetric unit, approximating two limit geometries, i.e. trigonal bipyramidal and square planar. This complex, like all copper–nitroxide complexes showing equatorial coordination,[6,14,23-25] is diamagnetic, presumably as a result of a strong antiferromagnetic interaction between unpaired electrons, due to a large overlap between magnetic orbitals.

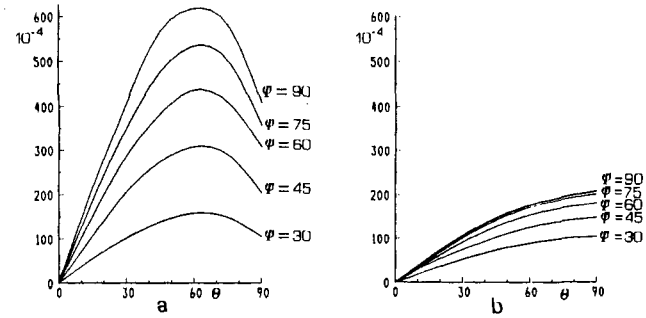

Figure 6. Variation of the absolute value of the overlap between magnetic orbitals with θ and ψ for $\phi = 0°$, in equatorially coordinated copper–nitroxide complexes: (a) square-planar case; (b) trigonal-bipyramidal case. The geometrical parameters are defined in the text.

In order to confirm this hypothesis, we performed extended Hückel calculations on two models approximating the two limit structures considered. The values of the different geometric parameters, extracted from the structures of several diamagnetic copper–nitroxide complexes, are reported in Table VI.

The extended Hückel calculations show that in both cases the magnetic orbital on the metal fragment is a linear combination of the d_{z^2} and $d_{x^2-y^2}$ atomic orbitals of copper. The variation of the absolute value of the overlap between the magnetic orbitals, as a function of the angular parameters, is very similar for square-planar and trigonal-bipyramidal geometries, even if, in the second case, the overlap S is always smaller. As shown in Figure 6, the overlap is very sensitive to the variations of ψ and θ, being in both cases an increasing function of ψ, between 0 and 90°, and varying with θ in such a way to reach a maximum around 60° for the square planar and at $\theta = 90°$ for the trigonal species. The dependence of the overlap on ϕ is much less pronounced: for example, when ϕ is varied from 0 to 90° for $\psi = 60°$ and $\theta = 30°$, the overlap varies from 6×10^{-4} to 7×10^{-4}, a very small variation in comparison with the strong dependence on ψ.

The geometrical parameters observed in real systems, reported in Table VI, are such that, for either square-pyramidal or square-planar complexes, θ is always very nearly 60°, while ψ varies between 60 and 90°. In this range of values there is a maximum of overlap between magnetic orbitals, which is about 2 orders of magnitude larger than that calculated for the axial complexes. Also in the trigonal bipyramid the overlap is always much higher than in the ferromagnetic systems, although in this case the difference is smaller than in the square-planar one. Therefore the observed diamagnetism of the complexes in Table VI appears to be justified. In summary the extended Hückel analysis shows that when the radical occupies an equatorial position it binds with a relatively strong bond to the metal, and the overlap is maximized. When on the other hand the radical occupies an axial positions, the bonding interaction is only weak, and the condition of maximum overlap does not apply.

Acknowledgment. Thanks are due to Dr. C. Zanchini, University of Florence, for recording the EPR spectra. The financial support of the Italian Ministry of Public Education and the CNR is gratefully acknowledged.

Registry No. $Cu(tfac)_2$, 14324-82-4; $Cu(tfac)_2$·NITMe, 112506-21-5.

Supplementary Material Available: Table SI (anisotropic thermal parameters) and Table SIII (parameters used in the extended Hückel calculations) (3 pages); Table SII (structure factor tables for $Cu(tfac)_2$·NITMe) (17 pages). Ordering information is given on any current masthead page.

(23) Dickman, M. H.; Doedens, R. J. *Inorg. Chem.* **1981**, *20*, 2677.
(24) Porter, L. C.; Dickman, M. H.; Doedens, R. J. *Inorg. Chem.* **1983**, *22*, 1962.
(25) Porter, L. C.; Doedens, R. J. *Inorg. Chem.* **1985**, *24*, 1006.